

Research Article: New Research | Neuronal Excitability

Non-Genomic Glucocorticoid Suppression of a Postsynaptic Potassium Current via Emergent Autocrine Endocannabinoid Signaling in Hypothalamic Neuroendocrine Cells following Chronic Dehydration

Postsynaptic glucocorticoid-cannabinoid signaling

Ning Wu¹ and Jeffrey G. Tasker^{1,2}

¹*Department of Cell and Molecular Biology, Tulane University, New Orleans, LA USA*

²*Tulane Brain Institute, Tulane University, New Orleans, LA USA*

DOI: 10.1523/ENEURO.0216-17.2017

Received: 21 June 2017

Revised: 19 August 2017

Accepted: 22 August 2017

Published: 5 September 2017

Author contributions: N.W. performed research; N.W. analyzed data; N.W. and J.G.T. wrote the paper; J.G.T. designed research.

Funding: HHS | NIH | National Institute of Neurological Disorders and Stroke (NINDS)
100000065
NS042081

Funding: HHS | NIH | National Institute of Mental Health (NIMH)
100000025
MH066958

Conflict of Interest: Authors report no conflict of interest.

HHS | NIH | National Institute of Neurological Disorders and Stroke (NINDS) [NS042081]; HHS | NIH | National Institute of Mental Health (NIMH) [MH066958].

Address for Correspondence: Jeffrey Tasker, Department of Cell & Molecular Biology, Tulane University, 6400 Freret St, New Orleans, LA 70117. Telephone: (504) 862-8726; Email: tasker@tulane.edu

Cite as: eNeuro 2017; 10.1523/ENEURO.0216-17.2017

Alerts: Sign up at eneuro.org/alerts to receive customized email alerts when the fully formatted version of this article is published.

Accepted manuscripts are peer-reviewed but have not been through the copyediting, formatting, or proofreading process.

Copyright © 2017 Wu and Tasker

This is an open-access article distributed under the terms of the Creative Commons Attribution 4.0 International license, which permits unrestricted use, distribution and reproduction in any medium provided that the original work is properly attributed.

**Non-Genomic Glucocorticoid Suppression of a Postsynaptic Potassium
Current via Emergent Autocrine Endocannabinoid Signaling in
Hypothalamic Neuroendocrine Cells Following Chronic Dehydration**

Ning Wu¹ and Jeffrey G. Tasker^{1,2}

¹Department of Cell and Molecular Biology and ²Tulane Brain Institute

Tulane University, New Orleans, LA, USA

Abbreviated title: Postsynaptic glucocorticoid-cannabinoid signaling

Address for Correspondence:

Jeffrey Tasker, Department of Cell & Molecular Biology, Tulane University, 6400 Freret St,
New Orleans, LA 70117; email: tasker@tulane.edu; telephone: (504) 862-8726

Key words: hypothalamus, HPA, glucocorticoid, magnocellular, CB1, osmolarity

Abstract: 232

Introduction: 410

Discussion: 1394

Acknowledgments: We would like to thank Dr. Katalin Smith for her expert technical assistance.

This work was supported by NIH grants NS042081 and MH066958, the Catherine and Hunter
Pierson Chair in Neuroscience, and the Tulane Research Enhancement Fund.

24 **ABSTRACT**

25 Glucocorticoids rapidly stimulate endocannabinoid synthesis and modulation of synaptic
26 transmission in hypothalamic neuroendocrine cells via a nongenomic signaling mechanism. The
27 endocannabinoid actions are synapse-constrained by astrocyte restriction of extracellular spatial
28 domains. Exogenous cannabinoids have been shown to modulate postsynaptic potassium
29 currents, including the A-type potassium current (I_A), in different cell types. The activity of
30 magnocellular neuroendocrine cells is shaped by a prominent I_A . We tested for a rapid
31 glucocorticoid modulation of the postsynaptic I_A in magnocellular neuroendocrine cells of the
32 hypothalamic paraventricular nucleus (PVN) using whole-cell recordings in rat brain slices.
33 Application of the synthetic glucocorticoid dexamethasone (Dex) had no rapid effect on the I_A
34 amplitude, voltage dependence, or kinetics in magnocellular neurons in slices from untreated rats.
35 In magnocellular neurons from salt-loaded rats, however, Dex application caused a rapid
36 suppression of the I_A and a depolarizing shift in I_A voltage dependence. Exogenously applied
37 endocannabinoids mimicked the rapid Dex modulation of the I_A and CB1 receptor antagonists
38 and agonists blocked and occluded the Dex-induced changes in the I_A , respectively, suggesting
39 an endocannabinoid dependence of the rapid glucocorticoid effect. Preincubation of control
40 slices in a gliotoxin resulted in the partial recapitulation of the glucocorticoid-induced rapid
41 suppression of the I_A . These findings demonstrate a glucocorticoid suppression of the
42 postsynaptic I_A in PVN magnocellular neurons via an autocrine endocannabinoid-dependent
43 mechanism, and suggest a possible role for astrocytes in the control of the autocrine
44 endocannabinoid actions.

45

46 **SIGNIFICANCE STATEMENT**

47 Stress causes elevated levels of glucocorticoid hormones and rapid and delayed glucocorticoid
48 feedback effects in the brain. Glucocorticoids regulate synaptic inputs to hypothalamic
49 neuroendocrine cells via a non-genomic release of endocannabinoid. We report a non-genomic
50 glucocorticoid modulation of a postsynaptic A-type potassium current in magnocellular neurons
51 via a novel autocrine endocannabinoid mechanism. The A-current modulation by glucocorticoids
52 occurred in neurons from rats subjected to chronic dehydration via salt loading, but not in
53 neurons from normally hydrated rats. Our findings suggest that chronic dehydration leads to an
54 glucocorticoid-induced endocannabinoid autocrine signaling in magnocellular neuroendocrine
55 cells. The neuroplastic mechanisms for this emergent signaling may be related to neuronal-glial
56 structural plasticity or to changes in rapid postsynaptic glucocorticoid and/or endocannabinoid
57 actions.

58

59 Osmotic challenge elicits a neuroendocrine stress response that results in an increase in
60 the circulating level of glucocorticoids (Roberts et al., 2011). Stress levels of glucocorticoids
61 cause endocannabinoid synthesis in PVN magnocellular and parvocellular neuroendocrine cells
62 (Di et al., 2003; Di et al., 2005a; Malcher-Lopes et al., 2006; Di et al., 2009). Endocannabinoids
63 are synthesized from lipid precursors in neuronal membranes and are released canonically as
64 retrograde signals to regulate the presynaptic release of glutamate and GABA (Di Marzo, 2011).
65 Endocannabinoid synthesis is elicited in magnocellular neuroendocrine cells of the hypothalamus
66 by depolarization (Hirasawa et al., 2004; Di et al., 2005b) and in response to oxytocin (Oliet et
67 al., 2007), as well as in response to rapid glucocorticoid actions (Di et al., 2003; Di et al., 2005a).
68 Glucocorticoid- and depolarization-induced retrograde endocannabinoid release from MNCs of
69 the hypothalamic paraventricular nucleus (PVN) and supraoptic nucleus causes a synapse-
70 specific suppression of glutamate release at excitatory synapses (Tasker, 2006; Tasker et al.,
71 2006). Restriction of the retrograde endocannabinoid actions exclusively to glutamate synapses
72 is controlled by astrocytes, since salt-loading-induced neuronal-glia plasticity and
73 pharmacologic inhibition of glial cell metabolism lead to spillover actions of endocannabinoids
74 at neighboring GABA synapses (Di and Tasker, 2013).

75 While endocannabinoids have been identified predominantly as retrograde messengers
76 that regulate presynaptic neurotransmitter release, they also have been reported to modulate
77 postsynaptic potassium channels (Deadwyler et al., 1995; Mackie et al., 1995; Schweitzer, 2000).
78 Glucocorticoids also have been shown to rapidly regulate postsynaptic properties by inhibiting
79 potassium currents in PVN neurons (Zaki and Barrett-Jolley, 2002) and hippocampal neurons
80 (French-Mullen, 1995; Olijslagers et al., 2008) and by modulating calcium-dependent potassium

81 channels in pituitary GH3 and AtT-20 cells (Huang et al., 2006). The mechanisms of these
82 postsynaptic actions of glucocorticoids have not been characterized.

83 The A-type potassium current (I_A) is a prominent voltage-gated conductance in PVN
84 magnocellular neurons that influences magnocellular neuron firing properties (Luther and Tasker,
85 2000; Ellis et al., 2007). Water deprivation or chronic salt loading induces dramatic structural
86 and functional plasticity among magnocellular neuroendocrine cells and astrocytes of the
87 hypothalamic PVN and supraoptic nucleus (Tasker et al., 2017). This plasticity results in
88 functional changes in magnocellular neuron electrical activity that leads generally to an increase
89 in excitability (Tasker et al., 2002). Here, we investigated whether glucocorticoids rapidly
90 modulate the I_A of magnocellular neurons in a transcription-independent fashion via putative
91 autocrine endocannabinoid signaling, and whether the rapid glucocorticoid modulation of the I_A
92 is altered with chronic osmotic stress via salt loading.

93

94 **Methods**

95 **Animals**

96 Male Sprague Dawley rats (5-6 weeks, Harlan, Indianapolis, IN) were used with the
97 approval of the Tulane University Animal Care and Use Committee and in accordance with
98 United States Public Health Service guidelines. Rats were dehydrated via chronic salt loading by
99 restricting them to drinking water with 2% NaCl for 6-8 days. Untreated control rats were age-
100 matched and were provided with regular tap drinking water.

101

102 **Hypothalamic slice preparation**

103 Rats were decapitated with a rodent guillotine under deep halothane anesthesia. The brain
104 was quickly removed and placed into ice-cold artificial cerebrospinal fluid (aCSF) containing (in
105 mM): 140 NaCl, 3 KCl, 1.3 MgSO₄, 1.4 NaH₂PO₄, 2.4 CaCl₂, 11 glucose, and 5 HEPES; the pH
106 was adjusted to 7.2–7.3 with NaOH, the osmolarity was 290–300 mOsm, and the aCSF was
107 bubbled with 100% oxygen. The hypothalamus was blocked and the caudal surface of the tissue
108 block was glued to the chuck of a vibrating tissue slicer. Two coronal hypothalamic slices 300
109 μ m in thickness and containing the PVN were sectioned, bisected at the midline, and submerged
110 in a holding chamber in oxygenated aCSF at room temperature, where they were allowed to
111 equilibrate for >1.5 hours before being transferred to a recording chamber.

113 **Electrophysiology**

114 Patch pipettes were pulled from borosilicate glass with a Flaming/Brown P-97
115 micropipette puller (Sutter Instruments, Novato, CA) to a tip resistance of 3–4 M Ω . They were
116 filled with a solution containing (in mM): 120 K-gluconate, 10 KCl, 1 NaCl, 1 MgCl₂, 1 EGTA,
117 2 Mg-ATP, 0.3 Na-GTP, and 10 HEPES; the pH was adjusted to 7.2 with KOH and the
118 osmolarity was adjusted to 300 mOsm with 20 mM D-sorbitol. For recordings, single hemi-slices
119 were transferred from the holding chamber to a submersion recording chamber, where they were
120 perfused with oxygenated aCSF at a rate of 2 ml/min and allowed to equilibrate for at least 15
121 min before starting the recordings. PVN neurons were visualized on a video monitor with a
122 cooled CCD camera using infrared illumination and differential interference contrast optics, and
123 were patch-clamped under visual control. After achieving the whole-cell configuration, the series
124 resistance was compensated by $\geq 60\%$ and the series resistance and whole-cell capacitance were

125 continuously monitored during experiments. Magnocellular neurons in the PVN were identified
126 based on their location, size, morphology and electrophysiological properties (i.e., prominent I_A
127 in voltage clamp and transient outward rectification in current clamp) (Tasker and Dudek, 1991;
128 Luther and Tasker, 2000). Recordings were performed using a Multiclamp 700A amplifier
129 (Molecular Devices, Sunnyvale, CA). Data were low-pass filtered at 2 kHz with the amplifier
130 and sampled at 10 kHz using the pClamp 9 data acquisition and analysis software package
131 (Molecular Devices, Sunnyvale, CA).

132 Prior to experiments, cells were tested in current-clamp mode and excluded from analyses if
133 they did not meet the following criteria: action potential amplitudes ≥ 50 mV from the threshold
134 to peak, an input resistance at resting potential of at least 500 M Ω , a resting membrane potential
135 negative to -50 mV, and a characteristic transient outward rectification (Tasker and Dudek, 1991;
136 Luther and Tasker, 2000). Slices were then bathed in aCSF with tetrodotoxin (TTX, 1 μ M) and
137 CdCl₂ (200 μ M) to block voltage-gated sodium channels and calcium channels, respectively, and
138 the recording configuration was switched to voltage clamp. The liquid junction potential
139 (calculated at 15 mV) was corrected *post hoc* during data analysis. All voltage-clamp recordings
140 were leak subtracted using a P/4 protocol. Series resistance compensation of $\geq 60\%$ was
141 routinely applied and changes in series resistance were monitored and compensated for
142 throughout the experiments. The series resistance at the beginning of recordings was less than 20
143 M Ω and recordings were discarded if changes in series resistance greater than 20% occurred
144 during the recordings.

145

146 **Voltage-dependence of activation and inactivation of the I_A and I_K**

147 We used two separate voltage protocols to isolate the I_A in PVN magnocellular neurons (Fig.
148 1A). The first protocol included a 200-ms hyperpolarizing conditioning step to -115 mV, which
149 removed the inactivation of the I_A , followed by sequential 200-ms depolarizing test pulses to
150 between -75 mV and +35 mV in 10-mV increments, which resulted in the activation of both the
151 I_A and I_K . The second protocol consisted of the same series of test pulses, but from a 200-ms
152 depolarizing conditioning step to -45 mV. The I_K was isolated from the I_A in the second protocol
153 because the I_A in magnocellular neurons is inactivated at -45 mV (Luther and Tasker, 2000). The
154 I_A was isolated by digitally subtracting the current responses generated by the second protocol
155 from those generated by the first protocol, which removed the I_K , leak current and capacitive
156 currents. The inactivation of the I_A was then studied with a third voltage protocol, consisting of
157 sequential 200-ms conditioning steps to between -135 mV and -25 mV in 10-mV increments,
158 which removed a variable amount of inactivation of I_A , followed by a command step to -15 mV.
159 We introduced a small step, to -75 mV for 5 ms, between the conditioning steps and the test steps
160 in both protocols, which allowed all test steps to be delivered from the same initial voltage level.
161 This way the voltage-clamp artifact was the same size and pulses were all more conveniently
162 subtracted from each other or compared. We tested the effect of this short pretest step on I_A and
163 did not observe it to change I_A significantly, since very little I_A was activated at -75 mV and 5 ms
164 was not sufficient to inactivate I_A (Luther and Tasker, 2000).

165

166 **Drug application**

167 Water-soluble forms of the steroids dexamethasone (dexamethasone-cyclodextrin complex,
168 Dex) (1 μ M) and corticosterone (corticosterone, 2-hydroxypropyl- β -cyclodextrin, 1 μ M) (Sigma-

169 Aldrich, St. Louis, MO) were directly dissolved in aCSF to their final concentrations and applied
170 in the bath perfusion. The Dex-bovine serum albumin (BSA) conjugate (10 μ M) was dissolved in
171 aCSF with 25% β -cyclodextrin (Sigma-Aldrich) as a carrier to increase its solubility. The
172 concentration of Dex-BSA (10 μ M) was selected to obtain an effective concentration of Dex of ~
173 1 μ M, as the BSA conjugate had a steroid-to-BSA ratio of 8:1. Tetrodotoxin (TTX, 1 μ M)
174 (Sigma-Aldrich) and CdCl₂ (200 μ M) (Sigma-Aldrich) were dissolved in sterile water and stored
175 in 10 mM stock solutions at -20°C, and were dissolved to their final concentrations in aCSF
176 immediately prior to bath application. The endogenous cannabinoids, anandamide (AEA) and 2-
177 arachidonoylglycerol (2-AG) (Tocris), were dissolved in DMSO and stored in 10 mM stock
178 solutions at -20°C, and were dissolved to their final concentrations in aCSF just before their
179 application in the bath. The cannabinoid receptor inverse agonists *N*-(piperidin-1-yl)-5-(4-
180 iodophenyl)-1-(2,4-dichlorophenyl)-4-methyl-1H-pyrazole-3-carboxamide (AM251) (1 μ M)
181 (Tocris) and rimonabant (SR141716, 1 μ M) (kindly provided by the NIMH Chemical Synthesis
182 and Drug Supply Program) were stored as 10 mM stock solutions in DMSO at -20°C and
183 dissolved to their final concentrations in aCSF before bath application. The vanilloid receptor
184 agonist, capsaicin (Tocris), and antagonist, capsazepine (Tocris), were stored as 10 mM stock
185 solutions in DMSO at -20°C and dissolved to their final concentrations in aCSF before bath
186 application. The protein synthesis inhibitor, cycloheximide (CHX) (Tocris) was dissolved in
187 sterile water and stored in a 10 mM stock solution at -20°C. Fluorocitrate (D,L-fluorocitric acid,
188 barium salt, 100 μ M) (Sigma) was dissolved in aCSF with 15 min of sonication. The DMSO and
189 β -cyclodextrin vehicles without the cannabinoids or glucocorticoids had no effect on the
190 waveform of the I_A.

191

192 **Statistical methods and curve fitting**

193 Values are expressed as means \pm standard errors of the mean. Statistical analyses were
194 performed using a two-way ANOVA with the Bonferroni multiple comparisons test for between-
195 group comparisons and the Student's paired *t* test for within-cell comparisons. Differences were
196 considered significant at $p < 0.05$. Boltzmann and exponential fits were used to fit data plots and
197 current traces using the fitting methods provided in the Graphpad Prism software (Graphpad
198 Software, La Jolla, CA) and Clampfit 9 (pCLAMP 9, Molecular Devices, Sunnyvale, CA),
199 respectively.

200

201 **Results**

202 **Rapid glucocorticoid modulation of I_A**

203 Corticosteroids rapidly modulate postsynaptic voltage-gated potassium currents in
204 hippocampal pyramidal neurons (Olijslagers et al., 2008). Magnocellular neuroendocrine cells of
205 the hypothalamic paraventricular nucleus (PVN) generate a prominent A-type potassium current
206 (I_A) that shapes their pattern of action potential firing (Luther and Tasker, 2000; Ellis et al.,
207 2007). We first tested for a rapid effect of glucocorticoids on the activation and inactivation of
208 the I_A in magnocellular neurons. The passive properties of the recorded magnocellular neurons
209 are presented in Table 1. The synthetic glucocorticoid dexamethasone (Dex), applied at a
210 concentration determined in previous studies to be near-saturating for rapid actions on synaptic
211 transmission (1 μ M) (Di et al., 2003; Di et al., 2016), had no effect on the I_A current. Based on a
212 two-way ANOVA ($p > 0.05$, $n = 9$), there was no change at the end of a 10-min bath application
213 of Dex in the I_A mean current amplitude, the I_A current density, or the voltage dependence of I_A
214 activation (Fig. 1B-E). Dex also had no effect on the activation kinetics of the I_A (10-90% rise

time measured with voltage steps from -115 mV to -25 mV; $p > 0.05$, Student's paired t test) (Fig. 1F) or on the voltage dependence of I_A inactivation ($p > 0.05$, two-way ANOVA) (Fig. 1G and H). The rate of inactivation was examined by fitting the I_A decay phase with a single exponential function to determine the inactivation time constant, which was also unchanged by Dex treatment (data not shown; $p > 0.05$, Student's paired t test). Dex had no effect on the amplitude, current density or voltage dependence of activation of I_K ($p > 0.05$, ANOVA; data not shown).

Chronic dehydration causes loss of glial coverage, enhanced glutamatergic, GABAergic and noradrenergic synaptic regulation of magnocellular neurons, and altered voltage-gated currents (Tasker et al., 2017). We next tested the possibility that glucocorticoid modulation of the I_A in PVN magnocellular neurons is altered under conditions of chronic dehydration caused by salt loading. Five to 7 days of salt loading caused an increase in the membrane capacitance and a decrease in the input resistance of magnocellular neurons (Table 1), which are characteristic of dehydration-induced hypertrophy in the magnocellular neurons (Miyata and Hatton, 2002; Di and Tasker, 2004; Shah et al., 2014). Unlike neurons from untreated rats, bath application of Dex (1 μ M) to PVN magnocellular neurons ($n = 15$) in slices from salt-loaded rats caused decreases in both the I_A current amplitude and the I_A current density ($p < 0.05$, 2-way ANOVA followed by the Bonferroni multiple comparisons test for each test step) (Fig. 2A-C) and shifted the activation curve of I_A positive by 4.9 mV ($p < 0.01$) (Fig. 4D) within 10 min. The I_A 10-90% rise time (Fig. 4E) and the voltage dependence of I_A inactivation (Fig. 4F, G) were unchanged. Like magnocellular neurons from untreated rats, Dex had no effect on the amplitude, current density, or voltage dependence of activation of I_K in magnocellular neurons recorded in slices from salt-loaded rats (data not shown).

238 The endogenous glucocorticoid corticosterone had a similar effect on the I_A activation in
239 MNCs from dehydrated rats. A 10-min bath application of corticosterone (1 μ M) reduced the I_A
240 mean current amplitude ($p < 0.01$, 2-way ANOVA, Bonferroni's test) (Fig. 3A) and induced a
241 4.3-mV positive shift in the I_A half-activation potential in MNCs from dehydrated rats ($p < 0.05$,
242 $n = 10$; Student's unpaired t test) (Fig. 3B). Corticosterone had no effect on the voltage
243 dependence of inactivation or on the inactivation time constant of I_A (data not shown).

244 Rapid glucocorticoid modulation of synaptic inputs to hypothalamic magnocellular and
245 parvocellular neuroendocrine cells are mediated by a membrane-associated receptor (Di et al.,
246 2003; Di et al., 2005a). Here, we investigated whether the rapid glucocorticoid modulation of the
247 I_A in PVN magnocellular neurons from dehydrated rats is also mediated by a membrane-
248 associated glucocorticoid receptor. Bath application of the membrane-impermeant Dex-bovine
249 serum albumin (Dex-BSA) conjugate (10 μ M), like Dex, reduced the mean current amplitude (p
250 < 0.01 , two-way ANOVA followed by Bonferroni multiple comparisons test for each test step, n
251 $= 7$) (Fig. 3C) and caused a 3.4-mV positive shift in the I_A half-activation potential ($p < 0.01$, $n =$
252 7 ; Student's unpaired t test) (Fig. 3D). This implicated a membrane site of steroid action. We
253 used a 10-fold higher concentration of Dex-BSA because the Dex-to-BSA ratio of the Dex-BSA
254 compound was 8 to 1, and we assumed that a single Dex molecule per Dex-BSA was available to
255 bind to the receptor. The weaker effect of the Dex-BSA compared to Dex could be due to a
256 lower effective concentration of available Dex to bind to the receptor or to a steric hindrance of
257 Dex binding by the Dex-BSA three-dimensional structure. We have shown recently that free
258 molecules of Dex do not dissociate from the Dex-BSA conjugate to penetrate into the cell (Weiss
259 et al., in press).

260 To determine whether the rapid glucocorticoid effect on I_A in MNCs from dehydrated rats
 261 is independent of *de novo* protein synthesis, we tested the sensitivity of the Dex effect to the
 262 protein synthesis inhibitor cycloheximide. Following a 30-min pre-incubation of slices in
 263 cycloheximide (10 μ M), the Dex-induced suppression of I_A amplitude ($p < 0.05$, two-way
 264 ANOVA, Bonferroni's *post-hoc* test, $n = 7$) (Fig. 3E) and positive shift in I_A half-activation
 265 potential (by 3.2 mV) ($p < 0.01$, $n = 7$; Student's unpaired *t* test) (Fig. 3F) within 10 min were
 266 maintained. This indicated that the Dex effect on I_A does not require protein synthesis and is
 267 mediated by a non-transcriptional mechanism.

268

269 **Endocannabinoid dependence of the glucocorticoid modulation of the I_A**

270 Rapid glucocorticoid modulation of glutamatergic synaptic inputs to magnocellular and
 271 parvocellular neuroendocrine cells of the hypothalamus are mediated by the retrograde release of
 272 an endocannabinoid (Di et al., 2003; Di et al., 2005a). Here, we tested for the endocannabinoid
 273 dependence of the rapid glucocorticoid modulation of the postsynaptic I_A in PVN magnocellular
 274 neuroendocrine cells from untreated rats. Bath application of the endocannabinoid 2-AG (1 μ M)
 275 caused a decrease in the mean I_A peak amplitude ($p < 0.05$, 2-way ANOVA, Bonferroni multiple
 276 comparisons test, $n = 16$) (Fig. 4A) and a 5-mV positive shift in the I_A half-activation potential
 277 ($p < 0.01$, Student's paired *t* test, $n = 16$) (Fig. 4B) in PVN magnocellular neurons. This effect of
 278 2-AG on the I_A was blocked by the CB1 receptor inverse agonist SR141716 (1 μ M, $n = 6$) (Fig.
 279 4C and D).

280 The other main endocannabinoid, anandamide (AEA), activates both CB1 receptors and
 281 transient receptor potential-vanilloid 1 (TRPV1) receptors (Marinelli et al., 2003; Derbenev et al.,
 282 2006), so we blocked TRPV1 receptors with the TRPV1 receptor antagonist capsazepine during

283 AEA application to test AEA modulation of I_A via activation of the CB1 receptor. Preapplication
284 of capsazepine (1 μ M) 10 min prior to AEA application had no effect on the I_A in magnocellular
285 neurons. AEA (1 μ M) added to the capsazepine in the bath solution caused a decrease in the I_A
286 peak amplitude ($p < 0.01$, 2-way ANOVA, Bonferroni multiple comparisons test, $n = 7$) (Fig. 4F)
287 and induced a 10-mV positive shift in the I_A half-activation potential ($p < 0.01$, Student's paired t
288 test, $n = 7$) (Fig. 4G). The TRPV1 agonist capsaicin (1 μ M) had no effect on the voltage
289 dependence of I_A activation (Fig. 4H). These data indicate that CB1 receptor activation with
290 endocannabinoids modulates I_A activation in a manner similar to glucocorticoids.

291 Unlike glucocorticoids, which had no effect on the I_A in magnocellular neurons from
292 normally hydrated rats, exogenously-applied endocannabinoids induced similar effects on the I_A
293 in magnocellular neurons from both normally hydrated and salt-loaded rats. Similar to
294 magnocellular neurons from untreated rats, exogenous application of 2-AG (1 μ M) to
295 magnocellular neurons from salt-loaded rats caused a significant decrease in the mean peak
296 current amplitude ($p < 0.05$, 2-way ANOVA, Bonferroni multiple comparisons test) and shifted
297 the activation curve of I_A to the right by 3.9 mV ($p < 0.05$, Student's paired t test) (compared to 5
298 mV in untreated rats). Exogenous application of the other main endocannabinoid, AEA (0.5 μ M),
299 also decreased the I_A peak amplitude ($p < 0.05$, 2-way ANOVA, Bonferroni multiple
300 comparisons test, $n = 11$), and shifted the I_A half-activation potential positive by 4.1 mV ($p <$
301 0.01, Student's paired t test, $n = 11$) in PVN magnocellular neurons from salt-loaded rats.

302 We next tested whether the postsynaptic modulation of the I_A by glucocorticoids in
303 magnocellular neuroendocrine cells from salt-loaded rats is dependent on CB1 receptor
304 activation. The CB1 receptor inverse agonists AM251 (1 μ M) and SR141716 (1 μ M) by
305 themselves had no effect on I_A amplitude or activation voltage dependence (data not shown), but

306 both AM251 and SR141716 blocked the Dex-induced decrease in I_A peak current amplitude (Fig.
 307 5A, C) and the rightward shift in the I_A activation curve (Fig. 5B, D) in MNCs in slices from
 308 salt-loaded rats, suggesting the involvement of endocannabinoid in the rapid glucocorticoid
 309 modulation of I_A .

310 We then tested whether glucocorticoids and endocannabinoids act through the same
 311 signaling pathway or through separate, parallel pathways, by testing for occlusion of the
 312 glucocorticoid-induced modulation of I_A by previous endocannabinoid exposure. In slices from
 313 salt-loaded rats, 2-AG applied alone caused a decrease in the I_A peak current amplitude ($p < 0.05$,
 314 2-way ANOVA, Bonferroni multiple comparisons test, $n = 4$) and a 5.5-mV positive shift in the
 315 I_A half-activation potential ($p < 0.05$, Student's paired t test, $n = 4$). The subsequent application
 316 of Dex (1 μ M), in the presence of 2-AG (1 μ M), failed to further decrease the peak I_A amplitude
 317 ($p > 0.05$; ANOVA) or to further shift the I_A half-activation potential to the right ($p > 0.05$,
 318 Student's paired t test, $n = 4$) (Fig. 5E). Similarly, AEA decreased the I_A peak current amplitude
 319 ($p < 0.05$, 2-way ANOVA, Bonferroni multiple comparisons test, $n = 4$) and shifted the I_A half-
 320 activation potential positive by 5-mV ($p < 0.05$, Student's paired t test, $n = 4$). Dex (1 μ M) failed
 321 to decrease the peak current amplitude further ($p > 0.05$; ANOVA) or elicit any further rightward
 322 shift in the I_A half-activation potential in the presence of AEA ($p > 0.05$, Student's paired t test, n
 323 = 4) (Fig. 5F).

325 **Possible glial regulation of the glucocorticoid modulation of I_A**

326 Chronic dehydration causes a structural change in astrocytic morphology that results in a
 327 reduction in the coverage of neurons and synapses by astrocytic processes (Miyata et al., 1994;
 328 Theodosis et al., 1995; Hatton, 1997; Tasker et al., 2017) and leads to spillover of synaptic

329 signals to extrasynaptic sites (Fleming et al.; Boudaba et al., 2003). We have found that salt
330 loading causes spillover of endocannabinoid from excitatory synapses to inhibitory synapses,
331 which was mimicked by suppressing glial activity with a gliotoxin (Di et al., 2013). The
332 emergence of rapid glucocorticoid modulation of the I_A with dehydration suggests a possible role
333 for glial coverage in the control of autocrine actions of endocannabinoids. To test for a role of
334 astrocyte buffering in the glucocorticoid-endocannabinoid modulation of I_A channels, we used
335 the gliotoxin fluorocitrate to impair astrocyte buffering capability. Fluorocitrate is preferentially
336 taken up by glia and blocks glial metabolic activity, including membrane transport, by inhibiting
337 the citric acid cycle (Clarke, 1991; Gordon et al., 2005). Slices from normally hydrated rats were
338 preincubated for approximately two hours in fluorocitrate (100 μ M). Dexamethasone (1 μ M) had
339 a small but significant effect on the I_A in PVN magnocellular neurons in slices from untreated
340 rats exposed to fluorocitrate. Whereas Dex had no effect on the I_A peak current amplitude
341 following fluorocitrate treatment ($p > 0.05$, ANOVA, $n = 8$) (Fig. 6A), it caused a small, but
342 significant, shift to the right in the I_A half-activation potential, by 3.2 mV ($p < 0.05$, Student's
343 paired t test, $n = 8$) (Fig. 6B). Thus, blocking glial metabolism in slices from untreated rats
344 partially reproduced the effect of *in-vivo* salt loading on the glucocorticoid modulation of the I_A .

346 Discussion

347 Glucocorticoids rapidly stimulate the synthesis and dendritic release of endocannabinoids,
348 which act retrogradely to modulate glutamate release from excitatory synaptic terminals onto
349 PVN neuroendocrine cells (Di et al., 2005b; Di et al., 2009). In addition to their well-
350 characterized presynaptic actions, cannabinoids have also been shown to modulate postsynaptic
351 potassium currents (Deadwyler et al., 1995; Tang et al., 2005), although, to our knowledge, the

352 regulation of postsynaptic conductances by endogenously released cannabinoids has not been
353 reported. Here, we demonstrate a glucocorticoid-induced suppression of the A-type potassium
354 current in hypothalamic magnocellular neuroendocrine cells that is CB1 receptor-dependent,
355 suggesting a postsynaptic autocrine action of endogenously-released cannabinoid. The
356 glucocorticoid modulation of I_A occurred rapidly, within minutes of its introduction, and reached
357 saturation within 10 minutes. The glucocorticoid effect was maintained with the membrane-
358 impermeant Dex-BSA conjugate, indicating that it was mediated by a membrane-associated
359 receptor, and it was not blocked by inhibiting protein synthesis, suggesting a nongenomic
360 mechanism. Therefore, like the rapid glucocorticoid effects on glutamate and GABA
361 neurotransmission in the PVN (Di et al., 2003; Di et al., 2009), these findings implicate a
362 membrane glucocorticoid receptor in the postsynaptic modulation of I_A .

363 We have performed concentration-response analyses on the rapid Dex- and
364 corticosterone-induced endocannabinoid production and retrograde suppression of excitatory
365 synaptic transmission in magnocellular neurons (Di et al.,). In those studies, we found that the
366 glucocorticoid-induced endocannabinoid synthesis in magnocellular neurons has a half-effective
367 concentration of approximately 350 nM and a saturating concentration near 1 μ M. We used the
368 near-saturating concentration of 1 μ M for Dex and corticosterone in this study to approximate
369 the high circulating glucocorticoid levels encountered following stress activation of the
370 hypothalamic-pituitary-adrenal (HPA) axis. The 1- μ M concentration of Dex and corticosterone
371 we used is equivalent approximately to 350-400 ng/mL of circulating glucocorticoid, which is
372 well within physiological limits. This concentration was ineffective in the magnocellular neurons
373 from untreated rats, which suggested that the effect seen in the magnocellular neurons from salt-
374 loaded rats was not the result of a non-specific action of the steroid.

375 We showed previously that glucocorticoids stimulate the synthesis of endocannabinoids
376 in the PVN (Malcher-Lopes et al., 2006), and that they suppress excitatory synaptic inputs to
377 PVN and SON neurons via the dendritic release and retrograde actions of endocannabinoids (Di
378 et al., 2003; Di et al., 2005a). Here we demonstrate the endocannabinoid dependence of the
379 glucocorticoid modulation of the I_A , which suggests that the glucocorticoid-induced release of
380 endocannabinoids also regulates postsynaptic conductances in these cells and is consistent with
381 cannabinoid modulation of I_A in other brain areas (Deadwyler et al., 1995; Tang et al., 2005). In
382 addition to their retrograde actions, therefore, glucocorticoid-induced endocannabinoids are
383 capable of acting in either an autocrine or a paracrine fashion to regulate postsynaptic potassium
384 currents in the PVN.

385 One possible mechanism of the negative modulation of the I_A by endocannabinoids is
386 that the activation of postsynaptic CB1 receptors triggers a change in the phosphorylation state of
387 the A-type potassium channels. There is a large body of evidence that supports modulation of I_A
388 by phosphorylation (Covarrubias et al., 1994; Birnbaum et al., 2004; Cai et al., 2005), and CB1
389 receptors are known to negatively couple via G_i to adenylyl cyclase activity, cAMP production
390 and PKA-dependent protein phosphorylation (Howlett et al., 2004). A decrease in the PKA-
391 dependent phosphorylation of Kv channel subunits may result in a decrease in the ability of the
392 voltage sensor of the I_A channel to respond to changes in membrane voltage (Park et al., 2006;
393 Yang et al., 2007). Another possibility is that CB1 receptor activation leads to the modulation of
394 one or more of the Kv channel auxiliary proteins, which are well known to regulate the I_A
395 (Covarrubias et al., 1994; Schrader et al., 2009).

396 The rapid glucocorticoid modulation of the I_A was seen only in magnocellular neurons
397 from rats subjected to chronic salt loading, a treatment known to induce the retraction of

398 astrocytic processes from around magnocellular neurons (Theodosis et al., 1995; Tasker et al.,
399 2017) and result in synaptic spillover of endocannabinoid from excitatory to inhibitory synapses
400 (Di et al., 2013). The emergent sensitivity to rapid glucocorticoid-induced endocannabinoid
401 modulation of the I_A could be caused either by dehydration-induced plasticity of postsynaptic
402 endocannabinoid or glucocorticoid signaling mechanisms or by the loss of glial endocannabinoid
403 buffering due to astrocytic retraction. The neuronal-glial structural plasticity in magnocellular
404 neurons under stimulated conditions (Theodosis et al., 1986; Miyata et al., 1994; Hatton, 1997) is
405 accompanied by increasing levels of ambient neurotransmitters, such as glutamate (Oliet et al.,
406 2001; Boudaba et al., 2003) and increasing heterosynaptic and extrasynaptic spillover of
407 neurotransmitters (Piet et al., 2004). We have found that the glutamate synapse-specific effects
408 of glucocorticoid-induced retrograde endocannabinoid actions (Di et al., 2009) are controlled by
409 glial coverage and that, following dehydration-induced glial retraction, endocannabinoid also
410 accesses and activates CB1 receptors on GABA synapses (Di et al., 2013). Our findings here are
411 consistent with autocrine glucocorticoid-induced endocannabinoid actions that are constrained
412 by glial restriction of extracellular endocannabinoid diffusion. That the I_A modulation by
413 exogenously applied cannabinoids was similar in slices from both untreated and salt-loaded rats
414 suggests that the lack of effect of endogenously released endocannabinoid in slices from
415 untreated rats was not due to a change in the sensitivity of endocannabinoid signaling with
416 dehydration. While these findings do not exclude the possibility of a change in the sensitivity to
417 rapid glucocorticoid signaling with salt loading, they may be explained by dehydration-induced
418 glial retraction that expands the extracellular diffusional reach of the endocannabinoid to allow
419 access to postsynaptic CB1 receptors that are normally inaccessible due to astrocytic coverage.
420 However, a role for astrocytes in limiting the glucocorticoid-induced autocrine endocannabinoid

actions is still speculative, as it was only partially supported by our recordings in slices in which glial metabolism, and thus endocannabinoid reuptake, was inhibited by the gliotoxin fluorocitrate (Clarke, 1991; Gordon et al., 2005). Thus, fluorocitrate treatment partially recapitulated the dehydration-induced facilitation of glucocorticoid modulation of the I_A , as Dex shifted the I_A activation curve but did not suppress the peak I_A following fluorocitrate preincubation. Therefore, further experiments are required to conclusively rule out possible plastic changes in glucocorticoid or endocannabinoid signaling in favor of the loss of astrocytic buffering to explain the emergence of rapid glucocorticoid modulation of the I_A with salt loading.

In magnocellular neurons from chronically dehydrated rats, we observed a glucocorticoid-induced decrease in the peak amplitude and rightward shift in the voltage dependence of activation of the I_A . The rightward shift in the activation curve of the I_A , with no change in the inactivation voltage dependence, means that a greater depolarizing stimulus is required to activate the transient potassium current and that fewer A-type potassium channels are activated with depolarization in the range of the action potential threshold. The lower peak amplitude of the I_A indicates that significantly less current will be activated with depolarization. The glucocorticoid modulation of the I_A , therefore, should increase the excitability of magnocellular neurons following chronic dehydration. Contrary to our expectations, Dex had no effect on spiking in neurons from salt-loaded rats. This may be because dehydration itself causes a reduction in the I_A current density (Wu and Tasker, unpublished observation), as well as changes in other voltage-gated conductances (Tanaka et al., 1999; Zhang et al., 2007), which makes it difficult to isolate the impact of glucocorticoid modulation of I_A on firing properties.

Glucocorticoid suppression of the I_A in magnocellular neurons during chronic dehydration should enhance the effect of synaptic excitation. Glucocorticoid-induced retrograde

444 endocannabinoid release suppresses presynaptic glutamate release and enhances presynaptic
445 GABA release onto magnocellular neurons from normally hydrated rats (Di et al., 2005a; Di et
446 al., 2009). This should negate any excitatory effect of suppressing the I_A ; however, the
447 glucocorticoid facilitation of GABA release is lost during dehydration due to the spillover
448 inhibitory actions of endocannabinoid at GABA synapses (Di et al., 2013). Therefore, the
449 excitation-inhibition balance established by glutamate and GABA release and I_A activation in the
450 dendrites would be tilted toward excitation. This combined with the increased sensitivity to
451 noradrenergic inputs (Di and Tasker, 2004) should enhance or maintain magnocellular neuron
452 activity and neurohypophyseal hormone release under conditions of osmotic stress (Hatton, 1997).
453 Collectively, the different effects of glucocorticoids on magnocellular neurons in untreated and
454 chronically dehydrated rats reveal a mechanism for the neuroendocrine system to respond to
455 stress and maintain homeostasis by means of integration of afferent neural circuit information
456 and circulating hormonal signals.

457

458

459

460 **List of References**

- 461 Birnbaum SG, Varga AW, Yuan LL, Anderson AE, Sweatt JD, Schrader LA (2004) Structure
462 and function of Kv4-family transient potassium channels. *Physiol Rev* 84:803-833.
- 463 Boudaba C, Linn DM, Halmos KC, Tasker JG (2003) Increased tonic activation of presynaptic
464 metabotropic glutamate receptors in the rat supraoptic nucleus following chronic
465 dehydration. *J Physiol* 551:815-823.
- 466 Cai SQ, Hernandez L, Wang Y, Park KH, Sesti F (2005) MPS-1 is a K⁺ channel beta-subunit
467 and a serine/threonine kinase. *Nature neuroscience* 8:1503-1509.
- 468 Clarke DD (1991) Fluoroacetate and fluorocitrate: mechanism of action. *Neurochem Res*
469 16:1055-1058.
- 470 Covarrubias M, Wei A, Salkoff L, Vyas TB (1994) Elimination of rapid potassium channel
471 inactivation by phosphorylation of the inactivation gate. *Neuron* 13:1403-1412.
- 472 Deadwyler SA, Hampson RE, Mu J, Whyte A, Childers S (1995) Cannabinoids modulate voltage
473 sensitive potassium A-current in hippocampal neurons via a cAMP-dependent process. *J*
474 *Pharmacol Exp Ther* 273:734-743.
- 475 Derbenev AV, Monroe MJ, Glatzer NR, Smith BN (2006) Vanilloid-mediated heterosynaptic
476 facilitation of inhibitory synaptic input to neurons of the rat dorsal motor nucleus of the
477 vagus. *J Neurosci* 26:9666-9672.
- 478 Di Marzo V (2011) Endocannabinoid signaling in the brain: biosynthetic mechanisms in the
479 limelight. *Nature neuroscience* 14:9-15.
- 480 Di S, Tasker JG (2004) Dehydration-induced synaptic plasticity in magnocellular neurons of the
481 hypothalamic supraoptic nucleus. *Endocrinology* 145:5141-5149.
- 482 Di S, Popescu IR, Tasker JG (2013) Glial control of endocannabinoid heterosynaptic modulation
483 in hypothalamic magnocellular neuroendocrine cells. *J Neurosci* 33:18331-18342.
- 484 Di S, Malcher-Lopes R, Halmos KC, Tasker JG (2003) Nongenomic glucocorticoid inhibition
485 via endocannabinoid release in the hypothalamus: a fast feedback mechanism. *J Neurosci*
486 23:4850-4857.
- 487 Di S, Maxson MM, Franco A, Tasker JG (2009) Glucocorticoids regulate glutamate and GABA
488 synapse-specific retrograde transmission via divergent nongenomic signaling pathways. *J*
489 *Neurosci* 29:393-401.
- 490 Di S, Malcher-Lopes R, Marcheselli VL, Bazan NG, Tasker JG (2005a) Rapid glucocorticoid-
491 mediated endocannabinoid release and opposing regulation of glutamate and gamma-
492 aminobutyric acid inputs to hypothalamic magnocellular neurons. *Endocrinology*
493 146:4292-4301.
- 494 Di S, Boudaba C, Popescu IR, Weng FJ, Harris C, Marcheselli VL, Bazan NG, Tasker JG
495 (2005b) Activity-dependent release and actions of endocannabinoids in the rat
496 hypothalamic supraoptic nucleus. *J Physiol* 569:751-760.
- 497 Ellis LD, Krahe R, Bourque CW, Dunn RJ, Chacron MJ (2007) Muscarinic receptors control
498 frequency tuning through the downregulation of an A-type potassium current. *J*
499 *Neurophysiol* 98:1526-1537.
- 500 ffrench-Mullen JM (1995) Cortisol inhibition of calcium currents in guinea pig hippocampal
501 CA1 neurons via G-protein-coupled activation of protein kinase C. *J Neurosci* 15:903-
502 911.

- 503 Fleming TM, Scott V, Naskar K, Joe N, Brown CH, Stern JE State-dependent changes in
 504 astrocyte regulation of extrasynaptic NMDA receptor signalling in neurosecretory
 505 neurons. *J Physiol* 589:3929-3941.
- 506 Gordon GR, Baimoukhametova DV, Hewitt SA, Rajapaksha WR, Fisher TE, Bains JS (2005)
 507 Norepinephrine triggers release of glial ATP to increase postsynaptic efficacy. *Nature*
 508 *neuroscience* 8:1078-1086.
- 509 Hatton GI (1997) Function-related plasticity in hypothalamus. *Annu Rev Neurosci* 20:375-397.
- 510 Hirasawa M, Schwab Y, Natah S, Hillard CJ, Mackie K, Sharkey KA, Pittman QJ (2004)
 511 Dendritically released transmitters cooperate via autocrine and retrograde actions to
 512 inhibit afferent excitation in rat brain. *J Physiol* 559:611-624.
- 513 Howlett AC, Breivogel CS, Childers SR, Deadwyler SA, Hampson RE, Porrino LJ (2004)
 514 Cannabinoid physiology and pharmacology: 30 years of progress. *Neuropharmacology*
 515 47 Suppl 1:345-358.
- 516 Huang MH, So EC, Liu YC, Wu SN (2006) Glucocorticoids stimulate the activity of large-
 517 conductance Ca^{2+} -activated K^{+} channels in pituitary GH3 and AtT-20 cells via a non-
 518 genomic mechanism. *Steroids* 71:129-140.
- 519 Luther JA, Tasker JG (2000) Voltage-gated currents distinguish parvocellular from
 520 magnocellular neurones in the rat hypothalamic paraventricular nucleus. *J Physiol* 523 Pt
 521 1:193-209.
- 522 Mackie K, Lai Y, Westenbroek R, Mitchell R (1995) Cannabinoids activate an inwardly
 523 rectifying potassium conductance and inhibit Q-type calcium currents in AtT20 cells
 524 transfected with rat brain cannabinoid receptor. *J Neurosci* 15:6552-6561.
- 525 Malcher-Lopes R, Di S, Marcheselli VS, Weng FJ, Stuart CT, Bazan NG, Tasker JG (2006)
 526 Opposing crosstalk between leptin and glucocorticoids rapidly modulates synaptic
 527 excitation via endocannabinoid release. *J Neurosci* 26:6643-6650.
- 528 Marinelli S, Di Marzo V, Berretta N, Matias I, Maccarrone M, Bernardi G, Mercuri NB (2003)
 529 Presynaptic facilitation of glutamatergic synapses to dopaminergic neurons of the rat
 530 substantia nigra by endogenous stimulation of vanilloid receptors. *J Neurosci* 23:3136-
 531 3144.
- 532 Miyata S, Hatton GI (2002) Activity-related, dynamic neuron-glial interactions in the
 533 hypothalamo-neurohypophysial system. *Microscopy research and technique* 56:143-157.
- 534 Miyata S, Nakashima T, Kiyohara T (1994) Structural dynamics of neural plasticity in the
 535 supraoptic nucleus of the rat hypothalamus during dehydration and rehydration. *Brain*
 536 *research bulletin* 34:169-175.
- 537 Oliet SH, Piet R, Poulain DA (2001) Control of glutamate clearance and synaptic efficacy by
 538 glial coverage of neurons. *Science* 292:923-926.
- 539 Oliet SH, Baimoukhametova DV, Piet R, Bains JS (2007) Retrograde regulation of GABA
 540 transmission by the tonic release of oxytocin and endocannabinoids governs postsynaptic
 541 firing. *J Neurosci* 27:1325-1333.
- 542 Olijslagers JE, de Kloet ER, Elgersma Y, van Woerden GM, Joels M, Karst H (2008) Rapid
 543 changes in hippocampal CA1 pyramidal cell function via pre- as well as postsynaptic
 544 membrane mineralocorticoid receptors. *Eur J Neurosci* 27:2542-2550.
- 545 Park KS, Mohapatra DP, Misonou H, Trimmer JS (2006) Graded regulation of the $\text{Kv}2.1$
 546 potassium channel by variable phosphorylation. *Science* 313:976-979.

- 547 Piet R, Vargova L, Sykova E, Poulain DA, Oliet SH (2004) Physiological contribution of the
548 astrocytic environment of neurons to intersynaptic crosstalk. *Proc Natl Acad Sci U S A*
549 101:2151-2155.
- 550 Roberts EM, Pope GR, Newson MJ, Lolait SJ, O'Carroll AM (2011) The vasopressin V1b
551 receptor modulates plasma corticosterone responses to dehydration-induced stress. *J*
552 *Neuroendocrinol* 23:12-19.
- 553 Schrader LA, Ren Y, Cheng F, Bui D, Sweatt JD, Anderson AE (2009) Kv4.2 is a locus for PKC
554 and ERK/MAPK cross-talk. *Biochem J* 417:705-715.
- 555 Schweitzer P (2000) Cannabinoids decrease the K(+) M-current in hippocampal CA1 neurons. *J*
556 *Neurosci* 20:51-58.
- 557 Shah L, Bansal V, Rye PL, Mumtaz N, Taherian A, Fisher TE (2014) Osmotic activation of
558 phospholipase C triggers structural adaptation in osmosensitive rat supraoptic neurons. *J*
559 *Physiol* 592:4165-4175.
- 560 Tanaka M, Cummins TR, Ishikawa K, Black JA, Ibata Y, Waxman SG (1999) Molecular and
561 functional remodeling of electrogenic membrane of hypothalamic neurons in response to
562 changes in their input. *Proc Natl Acad Sci U S A* 96:1088-1093.
- 563 Tang SL, Tran V, Wagner EJ (2005) Sex differences in the cannabinoid modulation of an A-type
564 K⁺ current in neurons of the mammalian hypothalamus. *J Neurophysiol* 94:2983-2986.
- 565 Tasker JG (2006) Rapid glucocorticoid actions in the hypothalamus as a mechanism of
566 homeostatic integration. *Obesity (Silver Spring)* 14 Suppl 5:259S-265S.
- 567 Tasker JG, Dudek FE (1991) Electrophysiological properties of neurones in the region of the
568 paraventricular nucleus in slices of rat hypothalamus. *J Physiol* 434:271-293.
- 569 Tasker JG, Di S, Boudaba C (2002) Functional synaptic plasticity in hypothalamic magnocellular
570 neurons. *Progress in brain research* 139:113-119.
- 571 Tasker JG, Di S, Malcher-Lopes R (2006) Minireview: rapid glucocorticoid signaling via
572 membrane-associated receptors. *Endocrinology* 147:5549-5556.
- 573 Tasker JG, Voisin DL, Armstrong WE (2017) 3.15 - The Cell Biology of Oxytocin and
574 Vasopressin Cells A2 - Pfaff, Donald W. In: *Hormones, Brain and Behavior* (Third
575 Edition) (Joëls M, ed), pp 305-336. Oxford: Academic Press.
- 576 Theodosis DT, el Majdoubi M, Gies U, Poulain DA (1995) Physiologically-linked structural
577 plasticity of inhibitory and excitatory synaptic inputs to oxytocin neurons. *Advances in*
578 *experimental medicine and biology* 395:155-171.
- 579 Theodosis DT, Chapman DB, Montagnese C, Poulain DA, Morris JF (1986) Structural plasticity
580 in the hypothalamic supraoptic nucleus at lactation affects oxytocin-, but not vasopressin-
581 secreting neurones. *Neuroscience* 17:661-678.
- 582 Yang JW, Vacher H, Park KS, Clark E, Trimmer JS (2007) Trafficking-dependent
583 phosphorylation of Kv1.2 regulates voltage-gated potassium channel cell surface
584 expression. *Proc Natl Acad Sci U S A* 104:20055-20060.
- 585 Zaki A, Barrett-Jolley R (2002) Rapid neuromodulation by cortisol in the rat paraventricular
586 nucleus: an in vitro study. *Br J Pharmacol* 137:87-97.
- 587 Zhang W, Star B, Rajapaksha WR, Fisher TE (2007) Dehydration increases L-type Ca(2+)
588 current in rat supraoptic neurons. *J Physiol* 580:181-193.

592 Figure Legends

593

594 **Figure 1. Dexamethasone had no rapid effect on I_A activation and inactivation in**

595 **magnocellular neurons from untreated rats.** A. Voltage-clamp protocol for isolating I_K and I_A .

596 Combined high-voltage-activated (I_K) and low-voltage-activated (I_A) currents were evoked by

597 stepping from a holding potential (V_h) of -115 mV to test steps of -75 mV to 35 mV in 10-mV

598 increments (left: voltage steps below, current responses above). High-voltage-activated

599 potassium current (I_K) was evoked by the same stepping protocol, except from a V_h of -45 mV

600 (middle: voltage steps below, current responses above). Subtraction of the currents activated

601 from a V_h of -45 mV from those activated from a V_h of -115 mV yielded the isolated low-

602 voltage-activated I_A (right current traces). B. Representative traces showing voltage-dependent

603 activation of I_A in PVN magnocellular neurons from untreated rats before and at the end of a 10-

604 min Dex application (1 μ M). Inset: activation voltage protocol. C. Plots of the mean current

605 amplitude of the I_A versus the test step potential, showing no effect of Dex on the I_A current

606 amplitude. D. Plots of the mean current density of the I_A (peak I_A /capacitance) versus the test

607 step potential, showing no effect of Dex on the I_A current density. E. Plots of the normalized

608 chord conductance of the I_A versus the test step potential, showing no effect of Dex on the

609 voltage dependence of activation of the I_A . F. Plots of the mean I_A 10-90% rise time vs. test step

610 potential; the Dex effect on the activation rate of I_A was not significant. G. Representative traces

611 showing voltage-dependent inactivation of I_A in response to voltage steps to -15 mV from 200-

612 ms conditioning steps between -135 mV and -25 mV before and after 10 min of DEX application

613 (1 μ M). Dexamethasone had no effect on the inactivation voltage dependence of the I_A . Inset:

614 inactivation voltage protocol. H. Plots of the mean normalized current amplitude versus the

615 conditioning step potential, showing no effect of DEX on the voltage dependence of I_A
616 inactivation. All recordings were in PVN magnocellular neurons in slices from untreated rats.

617

618 **Figure 2. Rapid glucocorticoid modulation of I_A in magnocellular neurons from salt-loaded**

619 **rats.** A. Representative traces showing voltage-dependent activation of I_A in PVN magnocellular

620 neurons from salt-loaded rats before and at the end of a 10-min DEX application (1 μ M). Inset:

621 activation voltage-clamp protocol. B. Plots of the mean peak amplitude of the I_A versus the test

622 step potential; Dex caused a significant reduction in the I_A current amplitude. C. Plots of the

623 mean current density (peak current/capacitance) of the I_A versus the test step potential; Dex

624 caused a significant reduction in the I_A current density. D. Plots of the normalized chord

625 conductance of the I_A versus the test step potential; Dex caused a significant shift to the right in

626 the voltage dependence of activation of the I_A . E. Plots of the mean 10-90% I_A rise time versus

627 the test step potential; Dex did not change the I_A activation kinetics. F. Representative traces

628 showing voltage-dependent inactivation of I_A in response to voltage steps to -15 mV from 200-

629 ms conditioning steps between -135 mV and -25 mV before and at the end of a 10-min Dex

630 application (1 μ M). Inset: inactivation voltage-clamp protocol. G. Plots of the mean normalized

631 current amplitude versus the conditioning potential. Dexamethasone had no effect on the voltage

632 dependence of I_A inactivation. All recordings were in PVN magnocellular neurons in slices from

633 salt-loaded rats. *, $p < 0.05$; **, $p < 0.01$ with ANOVA.

634

635 **Figure 3: The rapid glucocorticoid effect on I_A in magnocellular neurons from salt-loaded**

636 **rats was mediated by a membrane-associated receptor.** Plots of the mean current amplitude

637 of the I_A (A, C, E) and the I_A voltage dependence of activation (Normalized Chord Conductance)

638 (B, D, F) versus the test step potential before and at the end of a 10-min application of the

639 endogenous glucocorticoid corticosterone (Cort), the membrane-impermeant glucocorticoid Dex-
 640 BSA, and Dex in the presence of the protein translation inhibitor cycloheximide (CHX). The
 641 endogenous glucocorticoid, Cort (A, B), and the membrane-impermeant glucocorticoid, Dex-
 642 BSA (C, D, reduced the I_A peak amplitude and shifted the I_A voltage dependence to the right.
 643 Blocking protein synthesis (E, F) failed to block the glucocorticoid modulation of the I_A . *, $p <$
 644 0.05; **, $p < 0.01$ with ANOVA.

645
 646 **Figure 4. CB1 receptor agonists mimicked the glucocorticoid modulation of I_A .** A, B. Bath
 647 application of the endocannabinoid 2-AG (1 μ M) elicited a significant decrease in the I_A mean
 648 peak amplitude (A) and a positive shift in the I_A activation voltage dependence (Normalized
 649 Chord Conductance) (B) in magnocellular neurons from dehydrated rats. C, D. The CB1
 650 receptor inverse agonist SR141716 (rimonabant, 1 μ M) blocked the decrease in mean I_A peak
 651 amplitude (C) and the rightward shift in the chord conductance curve (D). E, F. Anandamide
 652 (AEA) elicited a decrease in the I_A mean peak amplitude (E) and a positive shift in the I_A
 653 activation voltage dependence (chord conductance) (F) in the presence of the TRPV1 receptor
 654 antagonist capsazepine (1 μ M). G. The TRPV1 agonist capsaicin (1 μ M) had no effect on the I_A
 655 voltage dependence of activation (chord conductance). *, $p < 0.05$; **, $p < 0.01$ with ANOVA.

656
 657 **Figure 5. CB1 receptor analogs blocked the glucocorticoid modulation of I_A .** A, B. The CB1
 658 receptor inverse agonist SR141716 (1 μ M) blocked the decrease in I_A peak amplitude (A) and
 659 the rightward shift in the voltage dependence of activation (Normalized Chord Conductance) (B)
 660 induced by Dex (1 μ M) in PVN magnocellular neurons in slices from salt-loaded rats. C, D. The
 661 CB1 receptor inverse agonist AM251 also blocked the Dex-induced decrease in I_A peak

662 amplitude (C) and the positive shift in activation voltage dependence (Normalized Chord
663 Conductance) (D) in PVN magnocellular neurons from salt-loaded rats. E, F. 2-AG (1 μ M) (E)
664 and AEA (1 μ M) (F) caused a positive shift in the I_A voltage-dependence curve (Normalized
665 Chord Conductance) from the control value, but subsequent application of Dex (1 μ M) failed to
666 further shift the curve, suggesting occlusion of the Dex effect by prior CB1 receptor activation. *,
667 $p < 0.05$ with ANOVA

668

669 **Figure 6. Glucocorticoid modulation of I_A following gliotoxin treatment.** Brain slices from
670 untreated rats were pre-incubated in the gliotoxin fluorocitrate for approximately two hours prior
671 to recordings. A. Following fluorocitrate treatment, Dex had no effect on the I_A mean peak
672 amplitude. B. Dex caused a positive shift in the voltage dependence of I_A activation (normalized
673 chord conductance) in fluorocitrate-treated slices. *, $p < 0.05$, ANOVA.

674

Table 1. Effects of chronic dehydration on passive electrical properties of magnocellular neurons.

	Untreated (n = 9)	Dehydrated (n = 15)
Membrane capacitance (pF)	24.3 \pm 2.5	40.0 \pm 4.4*
Membrane resistance (M Ω)	794.3 \pm 48.4	667.5 \pm 51.0*
Holding current (pA)	17.7 \pm 3.8	13.4 \pm 5.0*

*, $p > 0.05$ vs. neurons from untreated rats; Student's unpaired t test.

Fig. 1

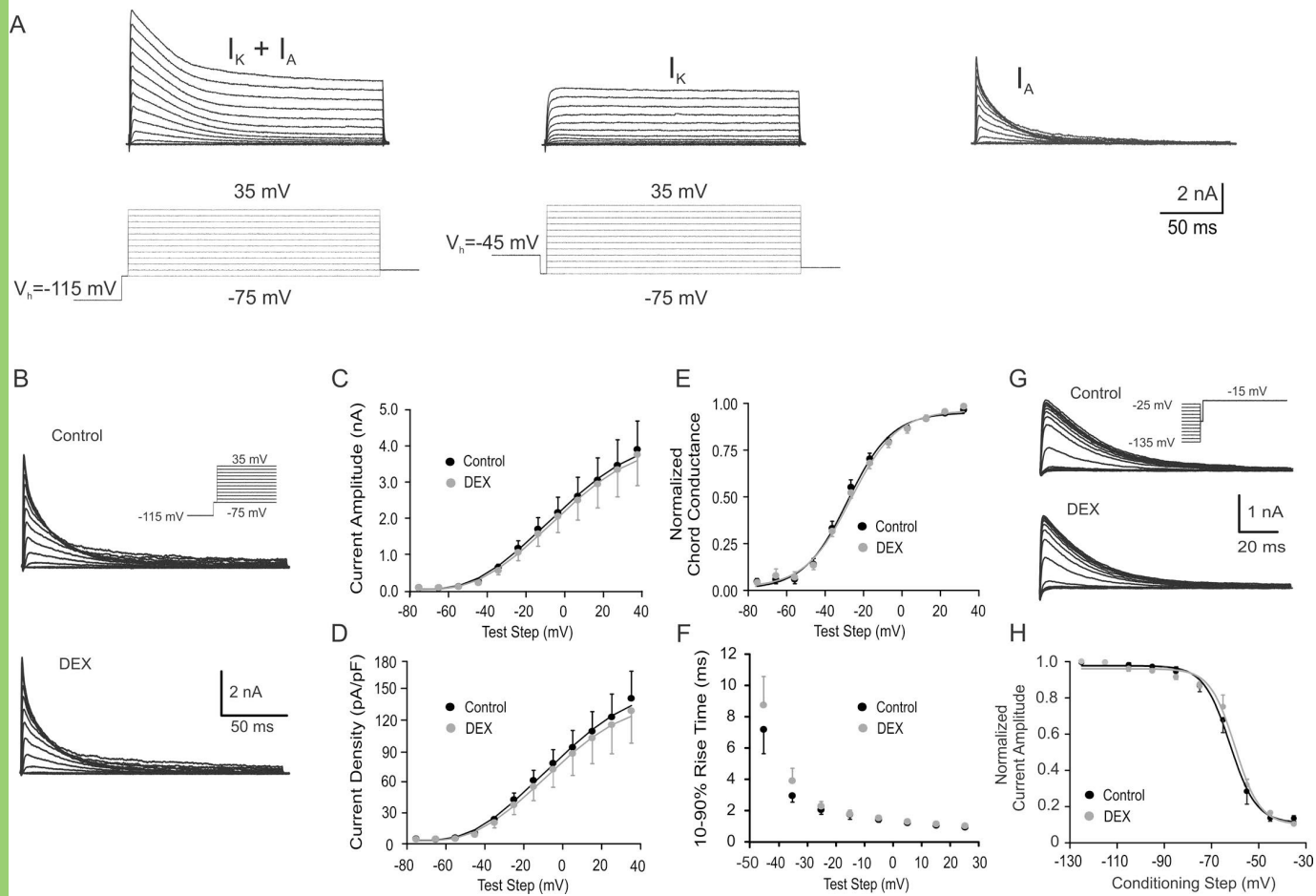


Fig. 2

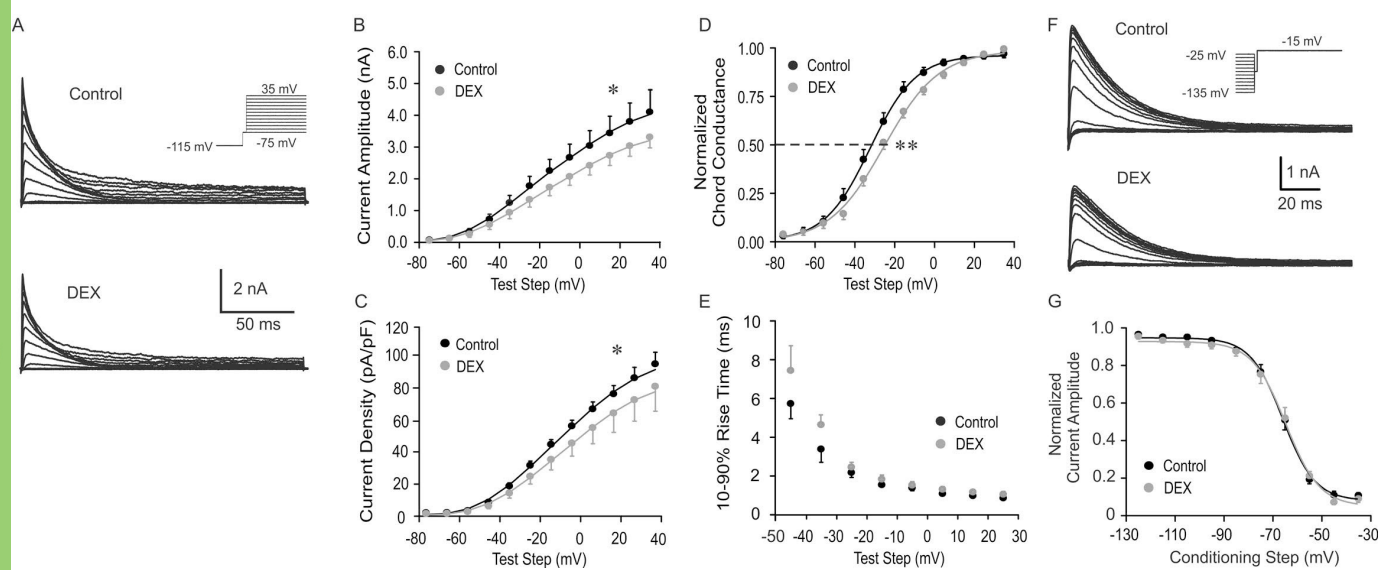


Fig. 3

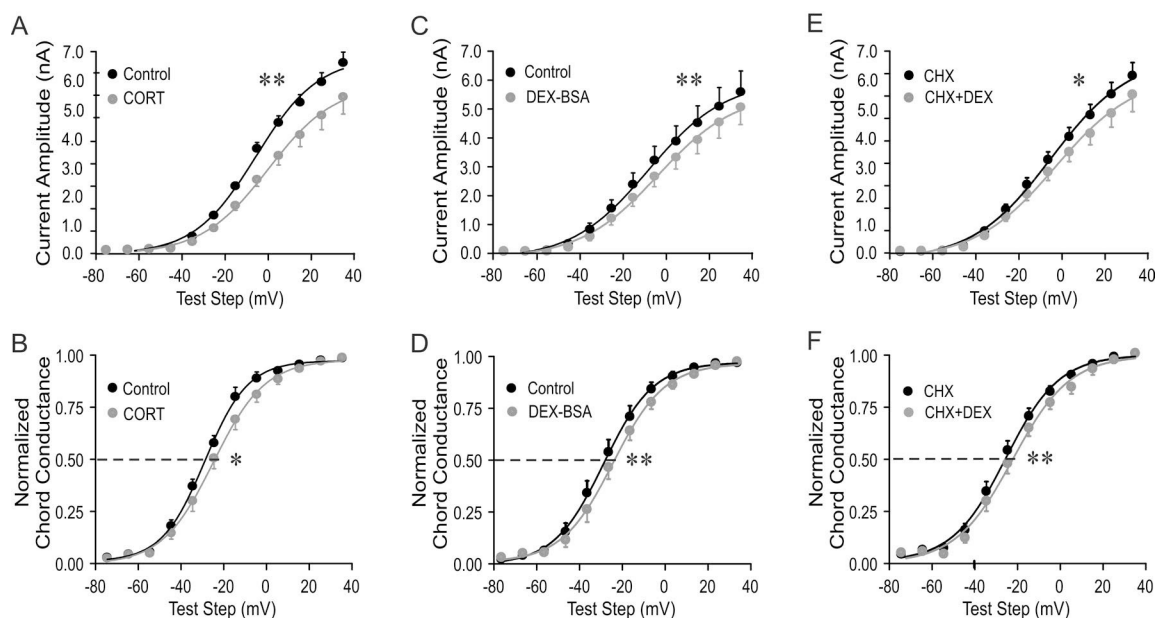


Fig. 4

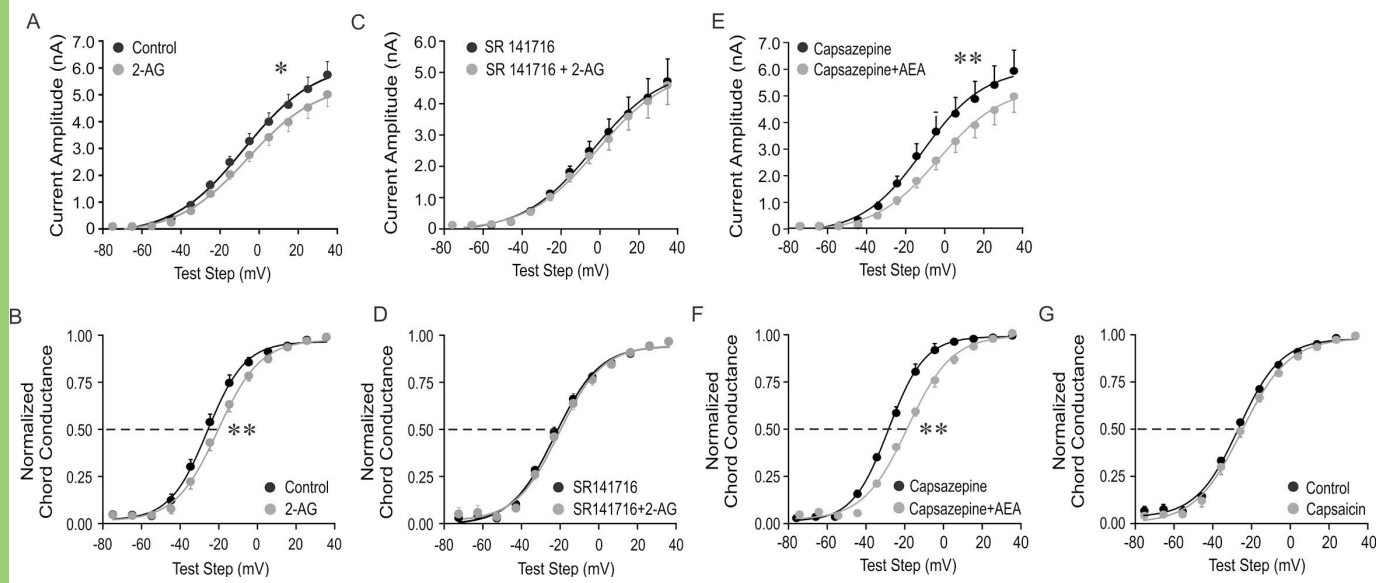


Fig. 5

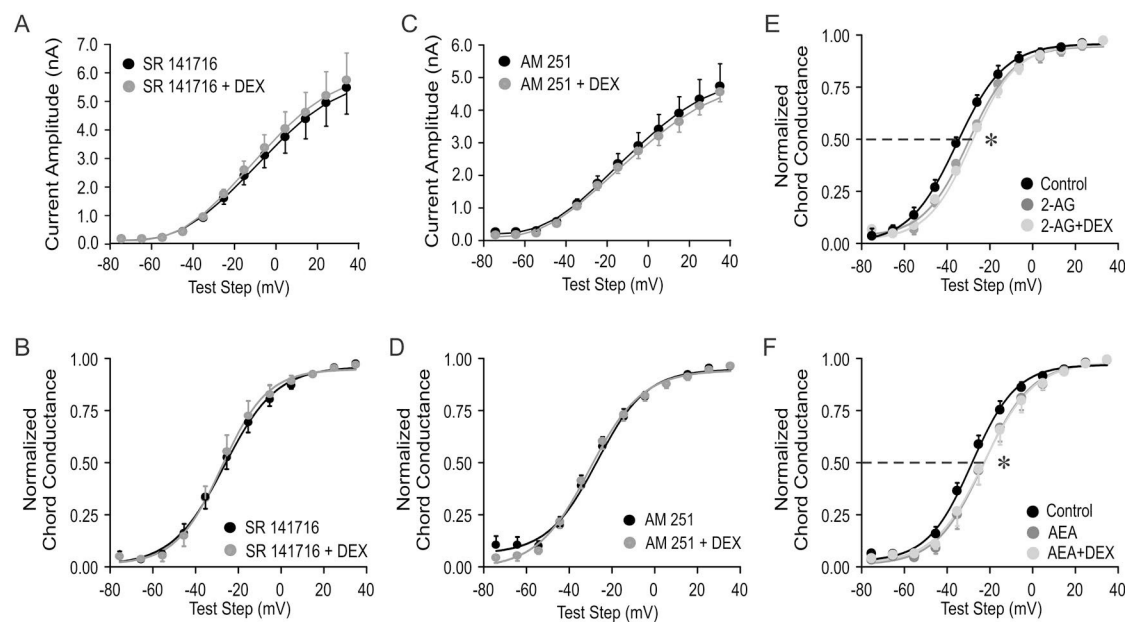


Fig. 6

